# NON-LINEAR LARGE DEFLECTION BENDING OF A CLAMPED SQUARE PLATE UNDER UNIFORM NORMAL PRESSURE

by

ARLENE M. HOFFMAN

A dissertation submitted to the Graduate Faculty in Mathematics in partial fulfillment of the requirements for the degree of Doctor of Philosophy, The City University of New York.

1974

This manuscript has been read and accepted for the Graduate Faculty in Mathematics in satisfaction of the dissertation requirement for the degree of Doctor of Philosophy.

May 2, 1974
date

Harry E. Rauch
Professor Harry E. Rauch
Chairman of Examining Committee

May 2, 1974
date

Richard Sacksteder
Professor Richard Sacksteder
Executive Officer

Professor Harry E. Rauch

Professor Richard Sacksteder

Professor Edgar Feldman
Supervisory Committee

The City University of New York

ACKNOWLEDGEMENTS

At this time I would like to extend my deepest appreciation to Professor Harry E. Rauch at whose suggestion I first began work on this problem. His encouragement, advice and continued interest in my research played a major role in the progress and completion of this dissertation.

A special note of thanks goes to Martin Hoffman for his invaluable help with several of the programming aspects of this research.

I would also like to acknowledge two agencies for their partial support during my years in graduate school: The National Science Foundation for their Graduate Traineeship and the Air Force Office of Scientific Research, Office of Aerospace Research, USAF, under Grant No. AFOSR 71-2063.

TABLE OF CONTENTS

# LIST OF TABLES

## LIST OF GRAPHS

## SYMBOLS USED

| | |
|---|---|
| $a$ | Length of sides |
| $h$ | Thickness |
| $u$ | Displacement of points in middle surface along x-axis |
| $v$ | Displacement of points in middle surface along y-axis |
| $w$ | Normal displacement (z-direction) of points in the middle surface |
| $p$ | Uniform normal pressure |
| $\nu$ | Poisson's ratio; taken here to be .3 |
| $E$ | Young's modulus |
| $D$ | $= E h^3 / 12(1-\nu^2)$; Flexural rigidity of plate |
| $\sigma'_x$ | Middle fiber stress in the x-direction |
| $\sigma'_y$ | Middle fiber stress in the y-direction |
| $\sigma''_x$ | Extreme fiber bending stress in the x-direction |
| $\sigma''_y$ | Extreme fiber bending stress in the y-direction |
| $\sigma_x$ | Total stress in extreme fiber in the x-direction |
| $\sigma_y$ | Total stress in extreme fiber in the y-direction |
| $p^*$ | $= p a^4 / E h^4$; Dimensionless pressure |
| $\delta$ | Normal deflection to thickness ratio |
| $p_x$ | Average middle fiber stress over middle surface in x-direction |
| $p_y$ | Average middle fiber stress over middle surface in y-direction |

## Section 1. Introduction

A theoretical analysis is presented for the elastic deflections and stresses of an initially flat square plate with clamped edges under uniform normal pressure. The situation considered may be called that of non-linear large-deflection bending. The four edge supports are assumed to clamp the plate in the sense that no rotations around the edges are possible, nor are deflections of the edges normal to the plane of the undeflected plate. In the case of movable edges each edge is free to move normal to itself in the plane of the plate, while in considering the case of fixed edges no motion of an edge normal to itself in the plane of the plate is possible. However, in both cases motion of points on an edge parallel to that edge is possible.

The plate is a rectangular parallelopiped with square cross section of side $a$ and thickness $h \ll a$. No prior assumption on the size of $a/h$ is made here, but typical values in the literature range from 100 to 200. The plate is assumed to be made of a homogeneous isotropic material which is elastic, i.e., which, when deformed by stresses within a certain range, returns to its initial undeformed state when the stresses are removed. Furthermore, it is assumed that within the elastic range for the material there is a sub-range within which Hooke's law is valid, i.e., the strains are linear functions of the stresses.

A plane section through the undeformed plate parallel to the square faces and midway between them is called the middle plane. A rectangular coordinate system will be attached to the plate by letting the middle plane be the $xy$ plane with origin at one corner and x- and y-axes parallel to the two adjacent edges. The z-axis is then erected normal to the $xy$ plane through the origin by the right hand rule. The two square surfaces of the plate then have the equations $z = \pm h/2$.

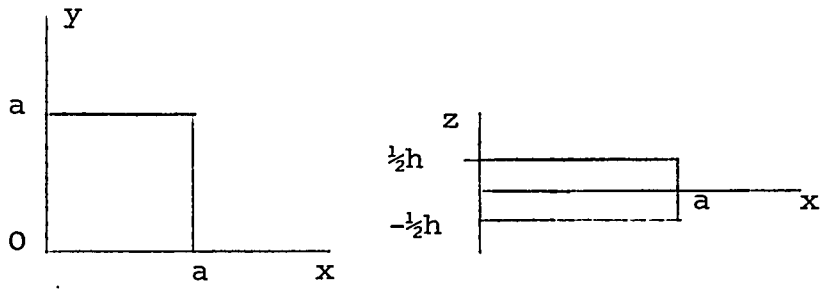


The theory assumes that each line segment of length $h$ normal to and bisected by the middle plane of the undeformed plate is mapped by the deformation isometrically onto a line segment of length $h$ in such a way that the image of the middle plane is the locus of the midpoints of the image segments in question, which are then normals to this locus. The locus is called the middle surface of the deformed plate. All of this assumption may be called the "Kirchhoff hypothesis" since it includes what is often given that name in the literature.

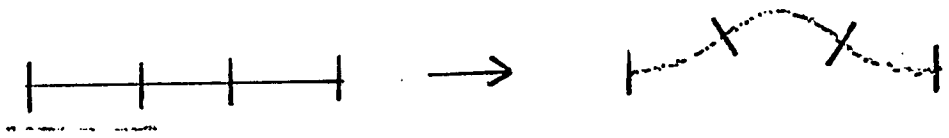

Using the Kirchhoff hypothesis one may give a complete description of the deformation of the plate by giving the displacement vector $(u,v,w)$, $u = u(x,y)$, $v = v(x,y)$, $w = w(x,y)$, whose initial point is the point $(x,y,0)$ in the middle plane of the undeformed plate and whose end point is its image $(x+u,y+v,w)$ on the middle surface under the deformation. The final assumption of the theory is that $u$ and $v$ and their derivatives are negligibly small compared to $w$ and its derivatives respectively, while all cubic or higher terms in all derivatives are negligible compared with lower degree terms. As a result the quadratic terms in the derivatives of $w$ are retained while the quadratic terms in the derivatives of $u$ and $v$, negligible in comparison, may be discarded. In particular, it is a reasonable approximation to visualize the point $(x,y,0)$ as being deflected to $(x,y,w)$.

It is sometimes stated that the theory is valid for normal deflections up to $h$, i.e., one thickness. However, here and elsewhere the theory seems to give reliable results (compared to experimental results) for a range of several thicknesses.

## Section 2. Equations and Boundary Conditions

The equations for non-linear deformation of flat plates are given by Föppl and von Kármán:

(a) (b)

$$\text{I:}\quad D\nabla^2\nabla^2 w = h\left[\frac{\partial^2\Phi}{\partial y^2}\frac{\partial^2 w}{\partial x^2} - 2\frac{\partial^2\Phi}{\partial x\partial y}\frac{\partial^2 w}{\partial x\partial y} + \frac{\partial^2\Phi}{\partial x^2}\frac{\partial^2 w}{\partial y^2}\right] + p$$

$$\text{II:}\quad \nabla^2\nabla^2\Phi = E\left[\left(\frac{\partial^2 w}{\partial x\partial y}\right)^2 - \frac{\partial^2 w}{\partial x^2}\frac{\partial^2 w}{\partial y^2}\right]$$

$\Phi$ is the middle surface stress function and is related to the middle surface stresses by:

$$\frac{\partial^2\Phi}{\partial x^2} = \sigma'_y\ ; \qquad \frac{\partial^2\Phi}{\partial y^2} = \sigma'_x\ ; \qquad -\frac{\partial^2\Phi}{\partial x\partial y} = \tau$$

The extreme fiber bending stresses are:

$$\sigma''_x = \frac{Eh}{2(1-\nu^2)}\left(\frac{\partial^2 w}{\partial x^2} + \nu\frac{\partial^2 w}{\partial y^2}\right); \qquad \sigma''_y = \frac{Eh}{2(1-\nu^2)}\left(\frac{\partial^2 w}{\partial y^2} + \nu\frac{\partial^2 w}{\partial x^2}\right)$$

The Föppl - von Kármán equations are both of fourth order and elliptic, and, therefore, a unique solution $(w,\Phi)$ ought to satisfy four boundary conditions on each of the edges. The definition of clamping given in Section 1, in fact, imposes the following boundary conditions:

(a) $w = 0 \quad x = 0, a; \qquad w = 0 \quad y = 0, a.$

This is the condition of no displacement normal to the middle plane at the edges.

(b) $\frac{\partial w}{\partial x} = 0 \quad x = 0, a; \qquad \frac{\partial w}{\partial y} = 0 \quad y = 0, a.$

This is the condition of no rotation about the edges (normal derivative vanishing).

(c) $\frac{\partial^2 \Phi}{\partial x \partial y} = 0 \quad x=0,a; \qquad \frac{\partial^2 \Phi}{\partial x \partial y} = 0 \quad y=0,a.$

This is the condition that the points on an edge can move parallel to that edge in the middle plane. Indeed, this implies that the tangential (shear) stress on each edge is zero, i.e., there is no force opposing the motion in question.

(d) i The condition of movable edges is expressed by:

$$\frac{\partial^2 \Phi}{\partial y^2} = 0 \quad x=0,a; \qquad \frac{\partial^2 \Phi}{\partial x^2} = 0 \quad y=0,a.$$

since these express the absence of normal in-plane forces on the edges.

(d) ii The conditions for fixed edges would be, strictly speaking,

$$u(0,y) = u(a,y) = 0; \qquad v(x,0) = v(x,a) = 0.$$

However, in the literature and here, these are replaced by the weaker conditions

$$u(a,y) - u(0,y) = \int_0^a \frac{\partial u}{\partial x}(x,y)\, dx = 0$$

$$v(x,a) - v(x,0) = \int_0^a \frac{\partial v}{\partial y}(x,y)\, dy = 0$$

of relatively fixed edges. However, the term fixed edges will be retained throughout this paper. The theory shows that this condition is given by III:

$$0 = \int_0^a \frac{\partial u}{\partial x}\, dx = \int_0^a \left[ \frac{1}{E} \frac{\partial^2 \Phi}{\partial y^2} - \frac{\nu}{E} \frac{\partial^2 \Phi}{\partial x^2} - \frac{1}{2} \left(\frac{\partial w}{\partial x}\right)^2 \right] dx$$

$$0 = \int_0^a \frac{\partial v}{\partial y}\, dy = \int_0^a \left[ \frac{1}{E} \frac{\partial^2 \Phi}{\partial x^2} - \frac{\nu}{E} \frac{\partial^2 \Phi}{\partial y^2} - \frac{1}{2} \left(\frac{\partial w}{\partial y}\right)^2 \right] dy$$

Section 3. Method of Solution

I represent the deflection, $w$, by the formal series $w(x,y) = \sum_i \sum_j f_{ij} w_{ij}(x,y)$. Here, $w_{ij}(x,y) = u_i(x)u_j(y)$ where $u_k(x)$ is Rayleigh's function, $R_k(x)$, defined on the interval $[0,a]$ and normalized to take the value 1 at $x = \frac{a}{2}$. $R_k$ is an eigenfunction of the linear differential equation for the displacements of a clamped rectangular bar,

$$\frac{d^4R}{dx^4}(x) = \lambda R(x); \qquad R = \frac{dR}{dx} = 0 \quad \text{at} \quad x = 0, a$$

corresponding to the eigenvalue $\lambda = m_k^4$, where $m_k$ is a root of $\cosh m_k \cos m_k - 1 = 0$.

$$R_k(x) = (\cos m_k - \cosh m_k)\left(\sinh \frac{m_k x}{a} - \sin \frac{m_k x}{a}\right) + (\sinh m_k - \sin m_k)\left(\cosh \frac{m_k x}{a} - \cos \frac{m_k x}{a}\right)$$

It is clear that the above choice of $w$ automatically fulfills boundary conditions (a) and (b) for the clamped plate since each term does.

The symmetry of the physical situation leads to the consideration of only those eigenfunctions $u_k(x)$ ( $u_k(y)$ ) which are themselves symmetric with respect to the line $x = \frac{a}{2}$ ( $y = \frac{a}{2}$ ). Since these are precisely the eigenfunctions with odd index, this means using only $w_{ij}$ with odd indeces; i.e., setting $f_{ij}$ equal to 0 if i or j is even. In addition, symmetry suggests that

the undetermined coefficients $f_{ij}$ and $f_{ji}$ be set equal to one another.

The first four odd eigenvalues, $m_1$, $m_3$, $m_5$, $m_7$, were computed to within $|\cosh m_k \cos m_k - 1| < 10^{-12}$. These eigenvalues and the corresponding values of $\cosh m_k$ and $\cos m_k$ are recorded here.

| m | cosh m | cos m |
|---|---|---|
| 4.730040744863 | $5.66545023831 \times 10^{1}$ | $.17650847 \times 10^{-1}$ |
| 10.99560783800 | $2.980587073805 \times 10^{4}$ | $.335504 \times 10^{-4}$ |
| 17.2787596574 | $1.5960260578711 \times 10^{7}$ | $.626556 \times 10^{-7}$ |
| 23.561944902 | $8.5465858254088 \times 10^{9}$ | $.117009 \times 10^{-9}$ |

The solution of the Föppl - von Kármán differential equations proceeds following the method of Formal Eigenfunction Expansion. The infinite series for w will be truncated after a finite number, n, of terms. This truncated series will be substituted into IIb, the right hand side of the stress equation, yielding terms involving products of derivatives of eigenfunctions. Each of these terms is expanded in a truncated series of eigenfunctions which contains exactly the same n functions as the original series representing w and coefficients of the same eigenfunctions are collected together.

Now one sees that each $w_{ij}$ also automatically fulfills boundary conditions (c) and (d)i. Hence, for the movable edge case, $\Phi$ is represented as an infinite series, $\Phi = \sum_i \sum_j g_{ij} w_{ij}$. I proceed as above and truncate the series after the same n terms. This series is substituted into IIa, the left hand side of the stress equation, and the resulting product of derivatives is again expanded in a series of the same n eigenfunctions. The left and right hand sides of II are then set equal, coefficient by coefficient, yielding n equations of the $g_{ij}$ in terms of $f_{rs}$. These equations are solved for $g_{ij}$ resulting in

$\Phi = \sum_i \sum_j g_{ij}(f_{rs}) w_{ij}$ (finite series).

This form of $\Phi$ together with the truncated series for $w$ is substituted into I. Products of derivatives are expanded in truncated series of the same n eigenfunctions as before, and the right and left hand sides of I are set equal, coefficient by coefficient. This yields n non-linear algebraic equations in the n unknowns, $f_{ij}$, which will be solved by various techniques in Section 8.

One finds by calculation that the forms of $w$ and $\Phi$ chosen above do not satisfy (d)ii, in particular, III. To remedy this, one treats II, with $w$ and hence the right side assumed as given, as an inhomogeneous linear partial differential equation, any solution of which can

be written as a sum of a particular solution, here $\Phi$, and a solution $\Phi_o$ of the associated homogeneous equation, i.e., $\nabla^2\nabla^2 \Phi_o = 0$. One then attempts for the given $w$ and $\Phi$ to find such a $\Phi_o$ so that (c) is satisfied by $\Phi + \Phi_o$, which means $\Phi_o$ since $\Phi$ already does, and so that III is satisfied by $\Phi + \Phi_o$, where it must be observed that III depends also on $w$. This last remark means that the boundary conditions in the fixed edge problem lead already to a source of coupled non-linearity distinct from that of the Föppl - von Kármán equations themselves.

One way to find such a $\Phi_o$ is to use a series expansion of the sort used in an analogous problem in Love [5], p. 494 (cf. also pp. 492-495) and truncate it to solve the boundary conditions (c) and III approximately. Here, however, a simpler one term approximation for $\Phi_o$ is suggested by the literature. This approximation satisfies (c) exactly, but III only approximately as indicated in Section 5. Despite the apparent crudity of this $\Phi_o$, very good agreement is obtained with the best results in the literature when its choice is coupled with the $w$ and $\Phi$ indicated, (see Section 9).

Namely, choose $\Phi_o = \frac{p_y}{2} x^2 + \frac{p_x}{2} y^2$, where the meaning of the constants $p_x$ and $p_y$ will be explained

below. Observe that one has $\frac{\partial^2 \Phi_o}{\partial x \partial y} = 0$, so that (c) is certainly satisfied. Observe further that $\Phi$ satisfies

$$\int_0^a \frac{\partial^2 \Phi}{\partial y^2}(x,y)\,dy = \Sigma\Sigma g_{ij} u_i(x)[u_j'(a) - u_j'(0)] = 0$$

for all $x$ and, hence,

$$\frac{1}{a^2}\iint \frac{\partial^2 \Phi}{\partial y^2}\,dx\,dy = 0$$

and similarly, $\frac{1}{a^2}\iint \frac{\partial^2 \Phi}{\partial x^2}\,dx\,dy = 0$.

Thus, $\Phi + \Phi_o$ satisfies

$$\frac{1}{a^2}\iint \frac{\partial^2(\Phi + \Phi_o)}{\partial y^2}\,dx\,dy = p_x$$

$$\frac{1}{a^2}\iint \frac{\partial^2(\Phi + \Phi_o)}{\partial x^2}\,dx\,dy = p_y$$

so that $p_x$ and $p_y$ are respectively the areal means over the plate of the middle fiber stresses in the $x$ and $y$ directions.

Notation Used in this Paper:

$$u_k'(x) = \frac{d\,u_k(x)}{\frac{d\,m_k x}{a}} = \frac{a}{m_k}\frac{d\,u_k(x)}{dx}$$

Thus, I will write $\frac{\partial^2 w_{11}}{\partial x \partial y} = \frac{m_1^2}{a^2} u_1'(x)\,u_1'(y)$, etc.

Section 4. <u>One Mode Solution: Movable Edges</u>

I assume the shapes $w = f_1 w_{11}$ and $\Phi = g_1 w_{11}$. The right hand side, IIb, of the stress equation contains the following terms:

$$\left[\frac{\partial^2 w}{\partial x \partial y}(x,y)\right]^2 = \frac{m_1^4}{a^4} f_1^2 \left[u_1'(x)\right]^2 \left[u_1(y)\right]^2$$

$$\frac{\partial^2 w}{\partial x^2}(x,y) = \frac{m_1^2}{a^2} f_1 u_1''(x) u_1(y)$$

$$\frac{\partial^2 w}{\partial y^2}(x,y) = \frac{m_1^2}{a^2} f_1 u_1(x) u_1''(y)$$

IIb can now be written as

$$E\left[\frac{m_1^4}{a^4} f_1^2 \left[u_1'(x)\right]^2 \left[u_1'(y)\right]^2 - \frac{m_1^4 f_1^2}{a^4} u_1(x) u_1''(x) u_1(y) u_1''(y)\right]$$

As a series in terms of $w_{11}$ alone, the coefficient of IIb is seen to be

$$\frac{E}{\int\int w_{11}^2} \left(\frac{m_1}{a}\right)^4 f_1^2 \left[ \textcircled{42}\,\textcircled{42} - \textcircled{3}\,\textcircled{3} \right]$$

Here (N) represents the value of a particular definite integral recorded in Table 7.

The left hand side, IIa, of the stress equation is

$$\nabla^2 \nabla^2 \Phi = \frac{\partial^4 \Phi}{\partial x^4} + 2 \frac{\partial^4 \Phi}{\partial x^2 \partial y^2} + \frac{\partial^4 \Phi}{\partial y^4} .$$

Upon substituting the assumed shape of $\Phi$ IIa becomes

$$2 \frac{m_1^4}{a^4} g_1 \left[ u_1(x) u_1(y) + u_1''(x) u_1''(y) \right] .$$

Expanding as a series in $w_{11}$ alone I obtain the coefficient

$$\frac{1}{\iint w_{11}^2} 2 \frac{m_1^4}{a^4} g_1 [ (39)(39) + (1)(1) ] .$$

Setting the coefficients of IIa and IIb equal to one another:

$$\frac{m_1^4}{a^4} E f_1^2 [ (42)(42) - (3)(3) ] = 2 \frac{m_1^4}{a^4} g_1 [ (39)(39) + (1)(1) ]$$

$$- .034211111 E f_1^2 = 2 g_1 ( .204725374)$$

$$g_1 = - .083553665 E f_1^2$$

Turning now to equation I, the right hand side takes the form

$$2 h \frac{m_1^4}{a^4} f_1 g_1 [u_1(x)u_1''(x)u_1(y)u_1''(y) - [u_1'(x)]^2[u_1'(y)]^2] + p.$$

Again I expand in terms of $w_{11}$ alone, obtaining the coefficient

$$\frac{1}{\iint w_{11}^2} [ 2 h \frac{m_1^4}{a^4} f_1 g_1 ( (3)(3) - (42)(42) ) + p (38)(38) ] .$$

The left hand side of I is, for my purposes, identical to that of II and upon substituting $w = f_1 w_{11}$, Ia becomes $\frac{E h^3}{12(1-\nu^2)} [ 2 \frac{m_1^4}{a^4} f_1 (u_1(x)u_1(y) + u_1''(x)u_1''(y)) ]$

Its $w_{11}$ coefficient is

$$\frac{1}{\iint w_{11}^2} \frac{E h^3}{12(1-\nu^2)} 2 \frac{m_1^4}{a^4} f_1 [ (39)(39) + (1)(1) ]$$

At this point I set the coefficient of Ia equal to that of Ib, obtaining

$$\frac{E h^3}{12(1-\nu^2)} 2 \frac{m_1^4}{a^4} f_1 \left[ (38)(38) + (1)(1) \right] =$$

$$2 h \frac{m_1^4}{a^4} f_1 g_1 \left[ (3)(3) - (42)(42) \right] + p (38)(38)$$

$$\frac{E h^3}{a^4} \left[ 18.7688874 \right] f_1 = - 2.8616875 \frac{E h}{a^4} f_1^3 + .27370095\, p$$

Dividing through by $\frac{E h^4}{a^4}$, I call $\delta_1 = f_1/h$ and

$p^* = \frac{p a^4}{E h^4}$, the dimensionless deflection and pressure

respectively, and obtain the final equation

$$68.5744\, \delta_1 + 10.4555\, \delta_1^3 = p^*$$

Section 5. <u>One Mode Solution: Fixed Edges</u>

Here again I assume the shape $w = f_1 w_{11}$. However, in view of the discussion in Section 3 regarding $\Phi$, I assume the shape $\Phi = g_1 w_{11} + p_x \frac{y^2}{2} + p_y \frac{x^2}{2}$, where $p_x$ and $p_y$ are constants yet to be determined. The fixed edge condition, III, now becomes

$$0 = \frac{m_1^2}{a^2 E} \int_0^a [g_1 u_1(x) u_1''(y) + p_x - \nu g_1 u_1''(x) u_1(y) - \nu p_y - \frac{E}{2} f_1^2 [u_1'(x)]^2 [u_1'(y)]^2 ] \, dx$$

Performing the x integration I obtain the result

$$p_x - \nu p_y = \frac{1}{a^3} [-m_1^2 g_1 \textcircled{38} u_1''(y) + \frac{E}{2} m_1^2 f_1 \textcircled{2} [u_1(y)]^2 ].$$

It follows from the symmetry of the horizontal and vertical edge conditions in III that $p_x - \nu p_y = p_y - \nu p_x$. From this one obtains $p_x(1 + \nu) = p_y(1 + \nu)$ and hence one sees that $p_x = p_y$.

At this point I am presented with the problem of approximating a function of y, namely the right hand side of the above equation, by the constant $p_x - \nu p_y$. The "least squares approximation", minimizing $\int_0^a [f(y) - c]^2 \, dy$, leads to evaluating c as the average value of f. Therefore I set

$$p_x - \nu p_y = \frac{1}{a} \int_0^a \frac{m_1^2}{a^3} [-g_1 \textcircled{38} u_1''(y) + \frac{E}{2} f_1^2 \textcircled{2} [u_1(y)]^2 ] \, dy.$$

Upon integrating, this equation becomes

$$p_x - \nu p_y = p_x(1-\nu) = \frac{E}{a^2} f_1^2 [.9669535]$$

and I find that $p_x = p_y = \frac{E}{a^2} f_1^2 [1.381362]$.

The choice of $\Phi = g_1 w_{11} + p_x \frac{y^2}{2} + p_y \frac{x^2}{2}$ leads to the addition of the terms

$$h \frac{m_1^2}{a^2} f_1 [ u_1''(x)u_1(y)p_x + u_1(x)u_1''(y)p_y ]$$

to the movable edge case of Ib. Expanding these terms in a series in $w_{11}$ alone, I obtain the coefficient

$$\frac{1}{\int\int w_{11}^2} \frac{Eh}{a^4} f_1^3 [-5.3428518].$$

The fixed edge equation then becomes

$$\frac{Eh^3}{a^4} f_1 [18.76888874] + \frac{Eh}{a^4} f_1^3 [8.2045393] = .27370095\, p .$$

Using the dimensionless deflection and pressure as before this equation takes the form

$$68.5744\, \delta_1 + 29.9763\, \delta_1^3 = p^* .$$

Section 6. Two Mode Solution: Movable Edges

Here $w$ is assumed to take the shape $w = f_{11}w_{11} + f_{13}(w_{13} + w_{31})$. Similarly, $\Phi$ is assigned the shape $g_{11} + g_{13}(w_{13} + w_{31})$. Following the identical procedure as in the one mode solution, I substitute the present expression for $w$ into IIb, obtaining

$$\frac{E}{a^4}\Big[\, m_1^4 f_{11}^2 [u_1'(x)]^2[u_1'(y)]^2 + m_1^2 m_3^2 f_{13}^2 \Big[ [u_1'(x)]^2[u_3'(y)]^2 + [u_3'(x)]^2[u_1'(y)]^2 + 2u_1'(x)u_3'(x)u_1'(y)u_3'(y) \Big] + 2 m_1^3 m_3 f_{11} f_{13} \Big[ [u_1'(x)]^2 u_1'(y)u_3'(y) + u_1'(x)u_3'(x)[u_1'(y)]^2 \Big] + m_1^4 f_{11}^2 u_1(x)u_1''(y)u_1(y)u_1''(y) - m_1^4 f_{11} f_{13} \Big[ u_1''(x)u_3(x)u_1(y)u_1''(y) + u_1(x)u_1''(x)u_1''(y)u_3(y) \Big] - m_1^2 m_3^2 f_{11} f_{13} \Big[ u_1''(x)u_1(x)u_1(y)u_3''(y) + u_1(x)u_3''(x)u_1(y)u_1''(y) \Big] \Big] .$$

Upon expanding as a series in $w_{11}$, $w_{13}$ and $w_{31}$ I calculate the resulting coefficients.

$w_{11}$ coefficient:

$$\frac{1}{\iint w_{11}^2}\frac{E}{a^2}\left[-17.124847 f_{11}^2 - 82.0783707 f_{11}f_{13} + 219.6646942 f_{13}^2\right]$$

$(w_{13} + w_{31})$ coefficient:

$$\frac{1}{\iint w_{13}^2}\frac{E}{a^2}\left[-20.519593 f_{11}^2 - 233.3758547 f_{11}f_{13} - 113.14013134 f_{13}^2\right]$$

Substituting the above expression for $\Phi$ into IIa results in

$$2\frac{m_1^4}{a^4} g_{11} u_1(x)u_1(y) + 2\frac{m_1^4}{a^4} g_{11} u_1''(x)u_1''(y)$$
$$+ \frac{m_1^4}{a^4} g_{13}[u_1(x)u_3(y) + u_3(x)u_1(y)]$$
$$+ \frac{m_1^4}{a^4} g_{13}[u_1(x)u_3(y) + u_3(x)u_1(y)]$$
$$+ 2\frac{m_1^2 m_3^2}{a^4} g_{13}[u_1''(x)u_3''(y) + u_3''(x)u_1''(y)] .$$

Expanding this expression as a series in the same three eigenfunctions I determine the following coefficients:

$w_{11}$ coefficient:

$$\frac{1}{\iint w_{11}^2}\frac{1}{a^2}\left[\, 204.95626501\, g_{11} + 85.02553688\, g_{13} \,\right]$$

$(w_{13} + w_{31})$ coefficient:

$$\frac{1}{\iint w_{13}^2}\frac{1}{a^2}\left[\, 42.51277104\, g_{11} + 3558.2053046\, g_{13} \,\right]$$

Equating IIa and IIb, coefficient by coefficient, one obtains two linear equations in $g_{11}$ and $g_{13}$. Solving for these quantities one finds

$$g_{11} = -.0815656\, E\, f_{11}^2 - .37511798\, E\, f_{11}f_{13} + 1.0903595\, E\, f_{13}^2$$
$$g_{13} = -.0047923\, E\, f_{11}^2 - .06110624\, E\, f_{11}f_{13} - .0448255\, E\, f_{13}^2$$

The assumed shapes of $w$ and $\Phi$ are substituted into the right hand side of I and the result will again be expanded as a series in terms of $w_{11}$, $w_{13}$ and $w_{31}$.

One may note at this point that the symmetry of the differential equation with respect to x and y eliminates over half of the calculations; i.e.

$w_{11}$ coefficient of $\frac{\partial^2 \Phi}{\partial y^2} \frac{\partial^2 w}{\partial x^2}$ =

$w_{11}$ coefficient of $\frac{\partial^2 \Phi}{\partial x^2} \frac{\partial^2 w}{\partial y^2}$

$w_{13}$ coefficient of $\frac{\partial^2 \Phi}{\partial y^2} \frac{\partial^2 w}{\partial x^2}$ =

$w_{31}$ coefficient of $\frac{\partial^2 \Phi}{\partial x^2} \frac{\partial^2 w}{\partial y^2}$

$w_{13}$ coefficient of $\frac{\partial^2 \Phi}{\partial x^2} \frac{\partial^2 w}{\partial y^2}$ =

$w_{31}$ coefficient of $\frac{\partial^2 \Phi}{\partial y^2} \frac{\partial^2 w}{\partial x^2}$

$w_{13}$ coefficient of $\frac{\partial^2 \Phi}{\partial x \partial y} \frac{\partial^2 w}{\partial x \partial y}$ =

$w_{31}$ coefficient of $\frac{\partial^2 \Phi}{\partial x \partial y} \frac{\partial^2 w}{\partial x \partial y}$

It is therefore sufficient to determine only the coefficients of $\frac{\partial^2 \Phi}{\partial y^2} \frac{\partial^2 w}{\partial x^2}$ as well as those of the mixed partial product $\frac{\partial^2 \Phi}{\partial x \partial y} \frac{\partial^2 w}{\partial x \partial y}$.

$$\frac{\partial^2 \Phi}{\partial y^2} = \frac{m_1^2}{a^2} g_{11} u_1(x) u_1''(y) + \frac{m_1^2}{a^2} g_{13} u_3(x) u_1''(y) + \frac{m_3^2}{a^2} g_{13} u_1(x) u_3''(y)$$

$$\frac{\partial^2 w}{\partial x^2} = \frac{m_1^2}{a^2} f_{11} u_1''(x) u_1(y) + \frac{m_1^2}{a^2} f_{13} u_1''(x) u_3(y) + \frac{m_3^2}{a^2} f_{13} u_3''(x) u_1(y)$$

$$\frac{\partial^2 \Phi}{\partial x \partial y} = \frac{m_1^2}{a^2} g_{11} u_1'(x) u_1'(y) + \frac{m_1 m_3}{a^2} g_{13} [u_1'(x) u_3'(y) + u_3'(x) u_1'(y)]$$

$$\frac{\partial^2 w}{\partial x \partial y} = \frac{m_1^2}{a^2} f_{11} u_1'(x) u_1'(y) + \frac{m_1 m_3}{a^2} f_{13} [u_1'(x) u_3'(y) + u_3'(x) u_1'(y)]$$

Therefore, one obtains:

$$\frac{\partial^2 \Phi}{\partial y^2}\frac{\partial^2 w}{\partial x^2} = \frac{m_1}{a} f_{11}g_{11}u_1(x)u_1''(x)u_1(y)u_1''(y)$$

$$+ \frac{m_1}{a} f_{13}g_{13}u_1''(x)u_3(x)u_1''(y)u_3(y)$$

$$+ \frac{m_1^2 m_3^2}{a} f_{13}g_{13}[u_1''(x)u_1(x)u_3(y)u_3''(y) + u_3(x)u_3''(x)u_1(y)u_1''(y)]$$

$$+ \frac{m_3}{a} f_{13}g_{13}u_1(x)u_3''(x)u_1(y)u_3''(y)$$

$$+ \frac{m_1}{a} f_{13}g_{11}u_1(x)u_1''(x)u_1''(y)u_3(y)$$

$$+ \frac{m_1^2 m_3^2}{a} f_{13}g_{11}u_1(x)u_3''(x)u_1(y)u_1''(y)$$

$$+ \frac{m_1}{a} f_{11}g_{13}u_1''(x)u_3(x)u_1(y)u_1''(y)$$

$$+ \frac{m_1^2 m_3^2}{a} f_{11}g_{13}u_1(x)u_1''(x)u_1(y)u_3''(y) \quad ;$$

$$\frac{\partial^2 \Phi}{\partial x \partial y}\frac{\partial^2 w}{\partial x \partial y} = \frac{m_1}{a} f_{11}g_{11}[u_1'(x)]^2[u_1'(y)]^2$$

$$+ \frac{m_1^2 m_3^2}{a} f_{13}g_{13}[\,[u_1'(x)]^2[u_3'(y)]^2 + [u_3'(x)]^2[u_1'(y)]^2 + 2\,u_1'(x)u_3'(x)u_1'(y)u_3'(y)\,]$$

$$+ \frac{m_1^3 m_3}{a} f_{11}g_{13}[\,[u_1'(x)]^2u_1'(y)u_3'(y) + u_1'(x)u_3'(x)[u_1'(y)]^2\,]$$

$$+ \frac{m_1^3 m_3}{a} f_{13}g_{11}[\,[u_1'(x)]^2u_1'(y)u_3'(y) + u_1'(x)u_3'(x)[u_1'(y)]^2\,] .$$

Expanding Ib as a series in $w_{11}$, $w_{13}$ and $w_{31}$, one finds the $w_{11}$ coefficient equal to:

$$2h \left[ w_{11} \text{ coefficient of } \frac{\partial^2 \Phi}{\partial y^2} \frac{\partial^2 w}{\partial x^2} - w_{11} \text{ coefficient of } \frac{\partial^2 \Phi}{\partial x \partial y} \frac{\partial^2 w}{\partial x \partial y} \right] + w_{11} \text{ coefficient of } p .$$

The coefficient of $(w_{13} + w_{31})$ involves slightly more consideration. The first four terms of $\frac{\partial^2 \Phi}{\partial y^2} \frac{\partial^2 w}{\partial x^2}$ are symmetric in x and y so that the $w_{13}$ and $w_{31}$ coefficients are equal. Since the identical situation occurs in the computation of $\frac{\partial^2 \Phi}{\partial x^2} \frac{\partial^2 w}{\partial y^2}$, one finds that a part of the $(w_{13} + w_{31})$ coefficient of $\frac{\partial^2 \Phi}{\partial y^2} \frac{\partial^2 w}{\partial x^2} + \frac{\partial^2 \Phi}{\partial x^2} \frac{\partial^2 w}{\partial y^2}$ results by merely doubling the $w_{13}$ coefficient of the above-mentioned four terms. The remaining part of the $(w_{13} + w_{31})$ coefficient can be most simply determined by computing the $w_{13}$ and $w_{31}$ coefficients of the last four terms of $\frac{\partial^2 \Phi}{\partial y^2} \frac{\partial^2 w}{\partial x^2}$ and then adding them together. Each term of $\frac{\partial^2 \Phi}{\partial x \partial y} \frac{\partial^2 w}{\partial x \partial y}$ is symmetric in x and y, and so its $(w_{13} + w_{31})$ coefficient is found by merely computing its $w_{13}$ coefficient. Finally, the $(w_{13} + w_{31})$ coefficient of the pressure, p, a constant, is simply $\frac{1}{\iint w_{13}^2} \frac{38}{6} p$ .

Using the above-determined expressions for $g_{11}$ and $g_{13}$ as quadratic functions of $f_{11}$ and $f_{13}$, as well as the table of integrals, I obtain cubic expressions of $f_{11}$ and $f_{13}$ in the coefficients of Ib. After combining like powers the coefficients become:

$w_{11}$ coefficient of Ib =

$$\frac{1}{\iint w_{11}^2}\left[\frac{E\,h}{a^2}\left[-3.1869415\, f_{11}^3 - 26.794766\, f_{11}^2 f_{13} - 25.6452393\, f_{11} f_{13}^2 + 68.572551\, f_{13}^3\right] + .27370095\, p\, a^2\right]$$

$(w_{13} + w_{31})$ coefficient of Ib =

$$\frac{1}{\iint w_{13}^2}\left[\frac{E\,h}{a^2}\left[-4.465795\, f_{11}^3 - 53.4907626\, f_{11}^2 f_{13} - 114.4623416\, f_{11} f_{13}^2 + 209.565523\, f_{13}^3\right] - .13535661\, p\, a^2\right]$$

The expansion of Ia as a series is identical to that of IIa, with $g_{ij}$ replaced by $f_{ij}$.

$w_{11}$ coefficient of Ia =

$$\frac{1}{\iint w_{11}^2}\frac{D}{a^2}\left[204.956265\, f_{11} + 85.02553688\, f_{13}\right]$$

$(w_{13} + w_{31})$ coefficient of Ia =

$$\frac{1}{\iint w_{13}^2}\frac{D}{a^2}\left[42.51277104\, f_{11} + 3558.20530463\, f_{13}\right]$$

Equating each of the coefficients of Ia and Ib I obtain two cubic equations in $f_{11}$ and $f_{13}$.

$$[A] \qquad \frac{E\,h^3}{a^4}\left[\,18.7688887\,f_{11} + 7.78622133\,f_{13}\,\right] =$$

$$\frac{E\,h}{a^4}\left[\,-3.18694154\,f_{11}^3 + 26.7947664\,f_{11}^2\,f_{13} - 25.64523934\,f_{11}\,f_{13}^2 + 68.57255096\,f_{13}^3\,\right] + .27370095\,p$$

$$[B] \qquad \frac{E\,h^3}{a^4}\left[\,3.8931109\,f_{11} + 325.8429766\,f_{13}\,\right] =$$

$$\frac{E\,h}{a^4}\left[\,-4.4657948\,f_{11}^3 - 53.490726\,f_{11}^2\,f_{13} - 114.4623416\,f_{11}\,f_{13}^2 + 209.56552309\,f_{13}^3\,\right] - .135356614\,p$$

I divide both equations by $\frac{E\,h^4}{a^4}$ times the respective coefficients of $p$. Once again, I call $\delta_{ij} = \frac{f_{ij}}{h}$ and $p^* = \frac{p\,a^4}{E\,h^4}$, the dimensionless deflections and pressure respectively. Solving the resulting equations for $p^*$ I obtain:

$$[A] \qquad 68.5744\,\delta_{11} + 28.4479\,\delta_{13} + 11.64388\,\delta_{11}^3 + 97.898\,\delta_{11}^2\,\delta_{13} + 93.698\,\delta_{11}\,\delta_{13}^2 - 250.5382\,\delta_{13}^3 = p^*$$

$$[B] \qquad -28.7619\,\delta_{11} - 2407.2927\,\delta_{13} - 32.9928\,\delta_{11}^3 - 395.184\,\delta_{11}^2\,\delta_{13} - 845.6354\,\delta_{11}\,\delta_{13}^2 + 1548.2474\,\delta_{13}^3 = p^*$$

Section 7. Two Mode Solution: Fixed Edges

At this point I investigate the two mode approximation under the fixed edge condition, III. One recalls that this edge condition requires the vanishing of

$$\int_0^a \left[ \frac{1}{E} \frac{\partial^2 \Phi}{\partial y^2} - \frac{\nu}{E} \frac{\partial^2 \Phi}{\partial x^2} - \frac{1}{2} \left(\frac{\partial w}{\partial x}\right)^2 \right] dx .$$

As was noted previously, the choice of $\Phi = g_{11}w_{11} + g_{13}(w_{13} + w_{31})$ will not satisfy this edge condition and so again I choose a first approximation to $\Phi$ by including the symmetric function $p_x \frac{y^2}{2} + p_y \frac{x^2}{2}$ . Proceeding in a manner identical to that of the one mode analysis, I obtain

$$\begin{aligned} 0 = a^2 \frac{1}{E} \int_0^a \Big[ & m_1^2 g_{11} u_1(x) u_1''(y) + m_1^2 g_{13} u_3(x) u_1''(y) \\ & + m_3^2 g_{13} u_1(x) u_3''(y) - \nu m_1^2 g_{11} u_1''(x) u_1(y) \\ & - \nu m_1^2 g_{13} u_1''(x) u_3(y) - \nu m_3^2 g_{13} u_3''(x) u_1(y) \\ & + p_x - \nu p_y \\ & - \frac{E}{2} \Big[ m_1^2 f_{11}^2 [u_1'(x)]^2 [u_1(y)]^2 + m_1^2 f_{13}^2 [u_1'(x)]^2 [u_3(y)]^2 \\ & \quad + m_3^2 f_{13}^2 [u_3'(x)]^2 [u_1(y)]^2 \\ & \quad + 2 m_1^2 f_{11} f_{13} [u_1'(x)]^2 u_1(y) u_3(y) \\ & \quad + 2 m_1 m_3 f_{11} f_{13} u_1'(x) u_3'(x) [u_1(y)]^2 \\ & \quad + 2 m_1 m_3 f_{13}^2 u_1'(x) u_3'(x) u_1(y) u_3(y) \Big] \Big] dx \end{aligned}$$

Integrating with respect to x, one determines

$$p_x - \nu p_y = p_x(1-\nu) =$$

$$\frac{1}{a^3}\Big[ - m_1^2 g_{11} (38)\, u_1''(y) - m_1^2 g_{13} (6)\, u_1''(y)$$
$$- m_3^2 g_{13} (38)\, u_3''(y) + \frac{E}{2} m_1^2 f_{11}^2 (2) [u_1(y)]^2$$
$$+ \frac{E}{2} m_1^2 f_{13}^2 (2) [u_3(y)]^2 + \frac{E}{2} m_3^2 f_{13}^2 (11) [u_1(y)]^2 \Big]$$

Upon computing the average value of this expression, $p_x$ is set equal to

$$1.381362 \frac{E}{a^2} f_{11}^2 + 2.4682766 \frac{E}{a^2} f_{11} f_{13} + 32.246964 \frac{E}{a^2} f_{13}^2 .$$

In light of the inclusion of $p_x \frac{y^2}{2} + p_y \frac{x^2}{2}$ in $\Phi$, the fixed edge case of Ib contains the movable edge terms, determined in Section 6, plus the additional terms:

$$\frac{h}{a^2}\Big[ p_x m_1^2 f_{11} u_1''(x) u_1(y) + p_x m_1^2 f_{13} u_1''(x) u_3(y)$$
$$+ p_x m_3^2 f_{13} u_3''(x) u_1(y) + p_y m_1^2 f_{11} u_1(x) u_1''(y)$$
$$+ p_y m_1^2 f_{13} u_3(x) u_1''(y) + p_y m_3^2 f_{13} u_1(x) u_3''(y) \Big]$$

$w_{11}$ coefficient of $p_x m_1^2 \frac{h}{a^2} f_{11} u_1''(x) u_1(y)$

$= w_{11}$ coefficient of $p_y m_1^2 \frac{h}{a^2} f_{11} u_1(x) u_1''(y) =$

$$\frac{E h}{a^4}\Big[ - 2.671426 f_{11}^3 - 4.773417 f_{11}^2 f_{13}^2 - 62.362629 f_{11} f_{13}^2 \Big]$$

$w_{13}$ coefficient of $p_x m_1^2 \frac{h}{a^2} f_{11} u_1''(x) u_1(y)$

$= w_{3i}$ coefficient of $p_y m_1^2 \frac{h}{a^2} f_{11} u_1(x) u_1''(y) = 0$

$w_{31}$ coefficient of $p_x m_1^2 \frac{h}{a^2} f_{11} u_1''(x)u_1(y)$

$= w_{13}$ coefficient of $p_y m_1^2 \frac{h}{a^2} f_{11} u_1(x)u_1''(y) =$

$$\frac{Eh}{a^4}\left[-2.3867086 f_{11}^3 - 4.2646724 f_{11}^2 f_{13} - 55.716098 f_{11} f_{13}^2\right]$$

$w_{11}$ coefficient of $p_x m_1^2 \frac{h}{a^2} f_{13} u_1''(x)u_3(y)$

$= w_{11}$ coefficient of $p_y m_1^2 \frac{h}{a^2} f_{13} u_3(x)u_1''(y) = 0$

$w_{13}$ coefficient of $p_x m_1^2 \frac{h}{a^2} f_{13} u_1''(x)u_3(y)$

$= w_{31}$ coefficient of $p_y m_1^2 \frac{h}{a^2} f_{13} u_3(x)u_1''(y) =$

$$\frac{Eh}{a^4}\left[-3.40843 f_{11}^2 f_{13} - 6.090328 f_{11} f_{13}^2 - 79.5674996 f_{13}^3\right]$$

$w_{31}$ coefficient of $p_x m_1^2 \frac{h}{a^2} f_{13} u_1''(x)u_3(y)$

$= w_{13}$ coefficient of $p_y m_1^2 \frac{h}{a^2} f_{13} u_3(x)u_1''(y) = 0$

$w_{11}$ coefficient of $p_x m_3^2 \frac{h}{a^2} f_{13} u_3''(x)u_1(y)$

$= w_{11}$ coefficient of $p_y m_3^2 \frac{h}{a^2} f_{13} u_1(x)u_3''(y) =$

$$\frac{Eh}{a^4}\left[-2.386709 f_{11}^2 f_{13} - 4.264672 f_{11} f_{13}^2 - 55.716098 f_{13}^3\right]$$

$w_{13}$ coefficient of $p_x m_3^2 \frac{h}{a^2} f_{13} u_3''(x)u_1(y)$

$= w_{31}$ coefficient of $p_y m_3^2 \frac{h}{a^2} f_{13} u_1(x)u_3''(y) = 0$

$w_{31}$ coefficient of $p_x m_3^2 \frac{h}{a^2} f_{13} u_3''(x) u_1(y)$

$= w_{13}$ coefficient of $p_y m_3^2 \frac{h}{a^2} f_{13} u_1(x) u_3''(y) =$

$$\frac{Eh}{a^4}\left[ - 27.401493 f_{11}^2 f_{13} - 48.962153 f_{11} f_{13}^2 - 639.669327 f_{13}^3 \right]$$

The terms due to the fixed edge condition therefore contribute the following to the coefficients of Ib:

$w_{11}$ coefficient:

$$\frac{2Eh}{a^4}\left[ - 2.67143 f_{11}^3 - 7.160126 f_{11}^2 f_{13} - 66.6273 f_{11} f_{13}^2 - 55.716098 f_{13}^3 \right]$$

$(w_{13} + w_{31})$ coefficient:

$$\frac{Eh}{a^4}\left[ - 2.38671 f_{11}^3 - 35.0746 f_{11}^2 f_{13} - 110.7686 f_{11} f_{13}^2 - 719.2368 f_{13}^3 \right]$$

Upon combining the coefficients of the movable case with those just determined I equate Ia and Ib obtaining, once again, two non-linear algebraic equations in $f_{11}$, $f_{13}$ and $p$.

$$[A] \quad \frac{Eh^3}{a^4}\left[ 18.7688887 f_{11} + 7.78622 f_{13} \right] =$$

$$\frac{Eh}{a^4}\left[ - 8.5298 f_{11}^3 - 41.11502 f_{11}^2 f_{13} - 158.8998 f_{11} f_{13}^2 - 42.8596 f_{13}^3 \right]$$

$$+ .27370095 p$$

$$[B] \quad \frac{Eh^3}{a^4}\left[\, 3.89311\, f_{11} + 325.84298\, f_{13} \,\right] =$$

$$\frac{Eh}{a^4}\left[ - 6.8525\, f_{11}^3 - 88.56536\, f_{11}^2 f_{13} - 225.2309\, f_{11} f_{13}^2 - 509.6713\, f_{13}^3 \right]$$

$$- .135356614\, p$$

Dividing both equations by $\frac{Eh^4}{a^4}$ times the respective coefficients of $p$ and calling $\delta_{ij} = \frac{f_{ij}}{h}$, $p^* = \frac{p a^4}{E h^4}$, I solve for $p^*$.

$$[A] \quad 68.5744\, \delta_{11} + 28.4479\, \delta_{13} + 31.1647\, \delta_{11}^3 + 150.2188\, \delta_{11}^2 \delta_{13} + 580.5599\, \delta_{11} \delta_{13}^2 + 156.5928\, \delta_{13}^3 = p^*$$

$$[B] \quad - 28.7619\, \delta_{11} - 2407.2927\, \delta_{13} - 50.6255\, \delta_{11}^3 - 654.3113\, \delta_{11}^2 \delta_{13} - 1663.9815\, \delta_{11} \delta_{13}^2 - 3765.3965\, \delta_{13}^3 = p^*$$

## Section 8. Numerical Solutions of the Two Mode Fixed Edge Equations

The end results of the preceding expansion methods yield two coupled cubic algebraic equations. My first attempt at a solution was quite naive and involved making a rough estimate for values of $\delta_{11}$ and $\delta_{13}$ and comparing the resulting values of $p^*$ in equations [A] and [B]. I initially assumed the magnitude of $\delta_{13}$ to be approximately 5% of that of $\delta_{11}$. Keeping the value of $\delta_{11}$ fixed, I altered the values of $\delta_{13}$ and noted the changes in $p^*$. Small increments in $\delta_{13}$ left [A] virtually unchanged. However, the effect of the larger coefficients in [B] was to appreciably alter $p^*$. I found that my fourth choice of $\delta_{13}$ usually led to values of $p^*$ in [A] and [B] which agreed to within the first decimal place. Upon closer inspection I found $|\delta_{13}|$ approximately 4.5% of $\delta_{11}$ for low pressures, ($p^* \approx 40$), $|\delta_{13}|$ approximately 7% of $\delta_{11}$ for $p^* \approx 150$, and $|\delta_{13}|$ approximately 9% of $\delta_{11}$ for $p^* \approx 350$.

I next tried to employ some type of iterative method. One such technique was as follows:

In [A], solve for $\delta_{11}^3$ in terms of everything else and then take the cube roots of both sides.

$$\delta_{11} = \sqrt[3]{\frac{p^*}{31.1647} - 2.2\,\delta_{11} - .913\,\delta_{13} - 4.82\,\delta_{11}^2\,\delta_{13} - 18.63\,\delta_{11}\,\delta_{13}^2 - 5.025\,\delta_{13}^3}$$

In [B], factor $\delta_{13}$ from each term containing it and then solve for $\delta_{13}$.

$$\delta_{13} = \frac{-(p^* + 28.7619\,\delta_{11} + 50.6255\,\delta_{11}^3)}{2407.2927 + 654.3113\,\delta_{11}^2 + 1663.9815\,\delta_{11}\,\delta_{13} + 3765.397\,\delta_{13}^3}$$

I proceeded to compute $\delta_{11}$ and $\delta_{13}$ corresponding to $p^* = 402$ using only an arithmetic calculator and a table of cube roots. Upon making an initial guess of $\delta_{11}^{(0)} = 2.2$ and $\delta_{13}^{(0)} = -.2$, I substituted these values into the right hand side of the $\delta_{11}$ equation and solved for $\delta_{11}^{(1)}$. At this time $\delta_{11}^{(1)}$ and $\delta_{13}^{(0)}$ are inserted into the right hand side of the $\delta_{13}$ equation and I obtain $\delta_{13}^{(1)}$. I then plugged the new values, $\delta_{11}^{(1)}$ and $\delta_{13}^{(1)}$ into the $\delta_{11}$ equation and the procedure is repeated until a reasonable convergence is achieved.

In the case of $p^* = 402$ each iteration served to confirm an additional decimal place of accuracy.

$\delta_{11}^{(1)} = \sqrt[3]{11.30812} \approx 2.244555$; $\delta_{13}^{(1)} = -.20344$

$\delta_{11}^{(2)} = \sqrt[3]{11.39855} \approx 2.250522$; $\delta_{13}^{(2)} = -.204053$

$\delta_{11}^{(3)} = \sqrt[3]{11.414795} \approx 2.25159$; $\delta_{13}^{(3)} = -.204155$

$\delta_{11}^{(4)} = \sqrt[3]{11.415159} \approx 2.251614$; $\delta_{13}^{(4)} = -.2041744$

$\delta_{11}^{(5)} = \sqrt[3]{11.415215} \approx 2.251617$; $\delta_{13}^{(5)} = -.20417485$

A very simple computer program may be devised to considerably shorten the time required for this procedure. For $p^* \geq 130$ I set $\delta_{11}$ and $\delta_{13}$ equal to 0 and proceeded with the iteration.

One important shortcoming to this method of iteration is that convergence seems to occur only for pressures, $p^*$, of magnitude greater or equal to about 130. In the case of smaller pressures one frequently obtains a negative cube root in solving for $\delta_{11}$, and this value will invariably lead to a divergent sequence. Convergence may be attained for smaller pressures if the initial choices of $\delta_{11}$ and $\delta_{13}$ are more accurate; the smaller the pressure, the greater the accuracy required. Unfortunately, the precision necessary for convergence with respect to pressures less than 100 is so great as to defeat the entire spirit of an iterative procedure.

Despite the problems encountered in the above method, the computation of deflections corresponding to pressures smaller than 100 can be accomplished by means of another iteration technique. In this present case I solve equation [B] as before, for $\delta_{13}$. This time, however, I solve equation [A] for $\delta_{11}$ in the same manner in which I just solved [B] for $\delta_{13}$. That is to say, I set

$$\delta_{11} = \frac{p^* - 28.4479\,\delta_{13} - 156.5928\,\delta_{13}^3}{68.5744 + 31.1647\,\delta_{11}^2 + 150.2188\,\delta_{11}\,\delta_{13} + 580.5599\,\delta_{13}^2}$$

For a given pressure, $p^* \leq 100$, I set $\delta_{11}^{(0)} = \delta_{13}^{(0)} = 0$. and inserted these values in the right hand sides of both equations, resulting in the new values, $\delta_{11}^{(1)}$ and $\delta_{13}^{(1)}$. These numbers are in turn substituted into the right hand sides of the two equations and the process is continued until the desired convergence is achieved for both equations.

One may be tempted to use this second iteration procedure for large pressures as well. It does still work for pressures less than or equal to 210; the greater the pressure, the slower the convergence. For example, requiring successive approximations to be within .0001 of each other made 10 iterations necessary for $p^* = 63.4$, 33 necessary for $p^* = 134.9$ and approximately 300 iterations necessary for $p^* = 210$.

Section 9. Discussion of Results

The bulk of this section will consist of an analysis of my fixed edge data and a comparison of these results with those of other researchers. However, I would first like to note the significant effects produced by imposing the fixed edge conditions on the formerly movable edge plate. The boundary conditions in the movable edge situation require that the stress, $\sigma_x' = \frac{\partial^2 \Phi}{\partial y^2}$, in the direction of the x-axis vanish on the edges $x = 0$ and $x = a$. (similarly, $\sigma_y' = \frac{\partial^2 \Phi}{\partial x^2}$, the stress in the direction of the y-axis, is to vanish on $y = 0$ and $y = a$.) The fixed edge condition imposes a non-zero stress, $\sigma_x' = p_x$ in this paper, at the boundaries. The presence of such a stress serves to increase the rigidity of the plate; for a given pressure the normal deflections, particularly at the center of the plate, are considerably smaller in the fixed edge case. Table I and the corresponding graphs in Figure I reveal this loss of flexibility as obtained in my two mode solutions of both the movable and fixed edge equations.

Fixed Edges

The normal displacements, $w$, are given in the one mode solution by $w = f_1 w_{11}$; in the two mode solution by $w = f_{11} w_{11} + f_{13}(w_{13} + w_{31})$. Since $w_{ij}(x,y)$ was

normalized to be 1 at the center of the plate, $(\frac{1}{2}a, \frac{1}{2}a)$, the central deflection is clearly equal to $f_1$ in the case of one mode and is equal to $f_{11} + 2f_{13}$ in the two mode approximation. A comparison of the one and two mode graphs of central deflection versus pressure can be found in Figure 2 and the corresponding Table 2. The one mode graph lies considerably above the two mode curve, indicating that the one mode solution results in a plate which is too flexible.

I attempted to improve the one mode solution by assuming a one mode shape for w, $w = f_{11}w_{11}$, while considering a two mode approximation for $\Phi$,

$$\Phi = g_{11}w_{11} + g_{13}(w_{13} + w_{31}) + \frac{p_x y^2}{2} + \frac{p_y x^2}{2} .$$

The resulting equation is easily obtained by referring to equation [A] of the two mode solution and setting $\delta_{13}$ equal to zero. The equation becomes

$$68.5744\,\delta_{11} + 31.1647\,\delta_{11}^3 = p^*$$

as compared to the one mode equation,

$$68.5744\,\delta_1 + 29.9763\,\delta_1^3 = p^* .$$

The cubic coefficient is increased slightly, but as can be seen once again from Figure 2 the difference between the two graphs is almost negligible.

I now consider the totality of stresses perpendicular to an edge acting at its midpoint. The symmetry of the plate guarantees the same results at each edge. As

mentioned earlier, the fixed edge condition imposes a stress, $\sigma_x' = \frac{\partial^2 \Phi}{\partial y^2} = p_x$, along the edge $x = 0$. The extreme fiber bending stress perpendicular to the edge $x = 0$ at its midpoint is given by $\sigma_x'' = \frac{Eh}{2(1-\nu^2)} \frac{\partial^2 w}{\partial x^2}$. Finally, the total stress perpendicular to the edge $x = 0$, denoted $\sigma_x$, is the sum $\sigma_x' + \sigma_x''$. The three stresses $\sigma_x'$, $\sigma_x''$ and $\sigma_x$ are non-dimensionalized by dividing each one by $\frac{Eh^2}{a^2}$ and are graphed versus dimensionless pressure, $p^*$, in Figure 3. (See also the corresponding Table 3.) It is seen that the bending stresses are quite large compared with the membrane stresses.

Much of the literature involving the bending of square plates deals with small deflections under uniform normal pressure; that is deflections which are small compared with the thickness of the plate. Under a small deflection hypothesis the stretching and shearing stresses in the middle surface are negligible, enabling one to neglect the non-linear terms in von Kármán's equations.

Consideration of the non-linear equation, as in this paper, is essential in any discussion of a plate with large deflections. Such analyses known to me have been given by Way [2], Levy [3] and Vol'mir [4], each employing distinct methods quite different from my own.

Levy's results, the most extensive of the three, include comparisons with Way's earlier work and, therefore, most of my own comparisons will be with Levy. Vol'mir

obtained a solution to the differential equations by approximating the shape of the deflected plate by $w = f \sin^2 \frac{\pi x}{a} \sin^2 \frac{\pi y}{a}$ which satisfies the boundary conditions of zero deflection and slope at the edges. His resulting equation in the fixed edge case is

$$71.4\,\delta + 35.9\,\delta^3 = p^* .$$

Here again, $\delta$ is the deflection to thickness ratio, $p^*$ is the dimensionless pressure.

Levy represents his deflection by the series $w = \Sigma\Sigma\ w_{mn} \sin \frac{m\pi x}{a} \sin \frac{n\pi y}{a}$, the general solution for the simply supported square plate with boundary conditions requiring the vanishing of the deflections and the edge bending moment per unit length at the edges. That is to say, $m_x = - D \left( \frac{\partial^2 w}{\partial x^2} + \nu \frac{\partial^2 w}{\partial y^2} \right)$ is to be zero along the edges $x = 0$ and $x = a$. ( Similarly, $m_y$ is to vanish on the edges $y = 0$ and $y = a$.)

In the clamped plate situation Levy was faced with exchanging the boundary conditions of zero bending moment for slope equal to zero at the edges. He accomplished this by expressing the edge moments as Fourier series with coefficients yet to be determined and incorporating these moments in an auxilliary pressure distribution. In the end he must solve several involved systems of equations relating his deflection, pressure and moment coefficients. Finally, convergence of the

deflection series to within three accurate decimal places requires series of 22 terms.

In Table 4 and the graph in Figure 4 Levy's 22 term solution and my two mode results for central deflection versus pressure are shown. The agreement is excellent for the smaller pressures and within 3% for the largest pressure.

I also find it interesting to compare the theoretical shapes of the deformed plate in terms of Levy's, Vol'mir's and my own distinct representations of $w$. For $p^* = 402$ I considered the plane section through the plate containing the line $y = \frac{a}{2}$, perpendicular to the $xy$ plane. The resulting middle surface deflection curves from $x = 0$ to $x = a$ are graphed in Figure 5 and one notes the remarkable agreement of my two mode shape with Levy's 22 term representation.

My stress results, however, do not agree quite as well with Levy's as the deflection data did. A comparison of my bending and middle membrane stresses with those of Levy can be found in Table 3 and the corresponding graphs in Figure 3. One observes that my membrane stresses, $\sigma_x'$, are too small, which was to be expected from the crude guess of $\Phi_o = \frac{p_x}{2} y^2 + \frac{p_y}{2} x^2$. It can be noted, however, that experimentally it is virtually impossible to clamp the edges so securely as to achieve perfectly fixed edges. In this case, my theoretical

results may not be too bad a reflection of the actual membrane stresses. My extreme fiber bending stresses can also be seen to be smaller than Levy's; at the largest pressure, $p^* = 402$, my bending stress differs from Levy's by 23%. It is important to note, however, that my one mode bending stresses are very much smaller than my two mode stresses, the difference at $p^* = 402$ being 37.5%. (See Table 6 and Figure 6.) This suggests that my bending stresses critically depend on the number of modes in the representation of $w$, and that even one additional mode would significantly improve these results.

Evaluation of Integrals

The final comments in this section deal with my attempts to evaluate the integrals occurring in the computation of the Fourier coefficients. The Rayleigh functions, being sums of products of sines, cosines and the hyperbolic functions sinh and cosh, have the property that upon expanding their derivatives as Fourier series in the original functions, the integrals involved in computing the Fourier coefficients are again sums of products of sin, cos, sinh, cosh. Each of these integrals can be computed in closed form, the formulas being found in almost any complete table of integrals. (See [7].) Using the values of $\cos m_1$ and $\cosh m_1$ listed earlier in this paper, the integrals occurring in the one mode

calculations can be easily computed using a twelve-place arithmetic calculator.

Difficulties arose, however, in the calculation of many of the integrals occurring in the two mode case. Certain of the integrals, such as $\int_0^a \sinh^4 \frac{m_3}{a}x \, dx$, have as many as 17 significant digits to the left of the decimal point. Evaluating a particular Fourier coefficient may involve additive cancellation of several numbers of such magnitudes. Since each Fourier coefficient turns out to be of absolute value less than 1, even with the aid of most computers, the significant digits to the right of the decimal point are all but lost and the resulting values of the coefficients are meaningless.

This obstacle in evaluating the coefficients in closed form led to the consideration of numerical approximation of these integrals. Instead of multiplying out an expression such as $[u_3(x)]^3 u_1(x)$ and integrating each of the resulting terms separately, I integrated the original product, $\int_0^a [u_3(x)]^3 u_1(x) \, dx$, using Simpson's rule with the number of intervals equal to $2^n$, n taking on integer values from 4 to 10. Recall that since the $u_j$'s were normalized to have maximum value 1, each function value in the computation will be less than or equal to 1. The convergence for $n = 10$ is correct to at least 8 decimal places for each of the 47 integrals.

Table 1. Two Mode Fixed and Movable Edges:
Central Deflection versus Pressure

| p* | Movable Edge Deflection | Fixed Edge Deflection |
|---|---|---|
| 17.79 | .2405 | .2361 |
| 38.3 | .5025 | .4699 |
| 50.0 | .64097 | .5818 |
| 63.4 | .7892 | .6937 |
| 80.0 | .9583 | .8132 |
| 95.0 | 1.0989 | .9070 |
| 134.9 | 1.4279 | 1.1111 |
| 184.0 | 1.770 | 1.3045 |
| 210.0 | 1.9315 | 1.3903 |
| 245.0 | 2.1330 | 1.4930 |
| 280.0 | 2.3200 | 1.5843 |
| 318.0 | 2.5098 | 1.6735 |
| 360.0 | 2.7065 | 1.7624 |
| 402.0 | 2.8918 | 1.8433 |

Figure 1. Two Mode Fixed and Movable Edges: Central Deflection versus Pressure

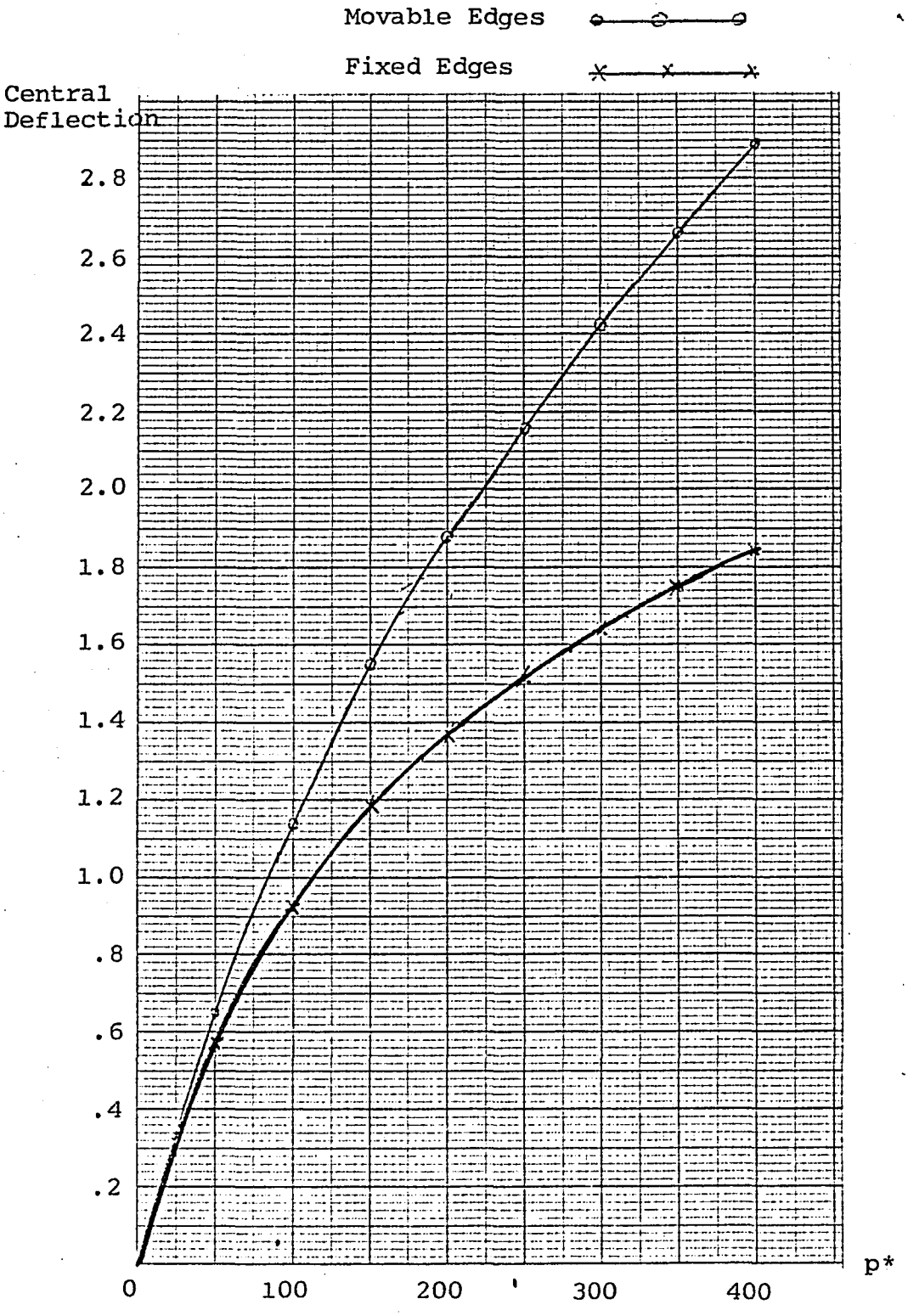

Table 2. Fixed Edge: Central Deflection versus Pressure

| p* | One Mode $w$ / One Mode $\Phi$ | One Mode $w$ / Two Mode $\Phi$ | Two Mode $w$ / Two Mode $\Phi$ |
|---|---|---|---|
| 17.79 | .2352 | .2344 | .2361 |
| 38.3 | .4643 | .4617 | .4999 |
| 50.0 | .5814 | .5775 | .5818 |
| 63.4 | .7064 | .7011 | .6937 |
| 80.0 | .8504 | .8434 | .8132 |
| 95.0 | .9722 | .9635 | .9070 |
| 134.9 | 1.2041 | 1.1939 | 1.1111 |
| 184.0 | 1.4232 | 1.4098 | 1.3045 |
| 210.0 | 1.5218 | 1.5070 | 1.3903 |
| 245.0 | 1.6410 | 1.6245 | 1.4930 |
| 280.0 | 1.7481 | 1.7300 | 1.5843 |
| 318.0 | 1.8535 | 1.8340 | 1.6735 |
| 360.0 | 1.9597 | 1.9386 | 1.7624 |
| 402.0 | 2.0571 | 2.0346 | 1.8433 |

Figure 2. Fixed Edge: Central Deflection versus Pressure

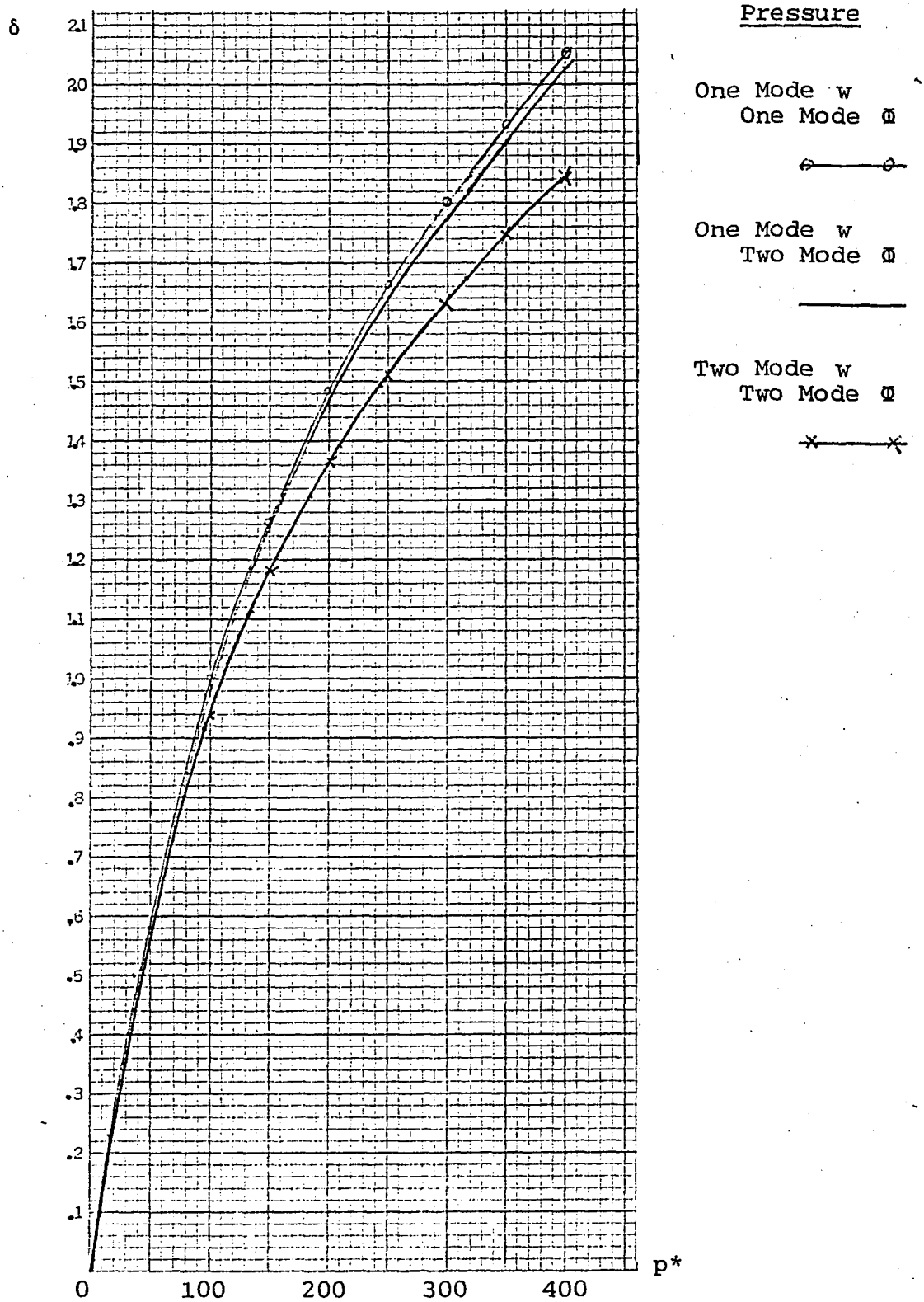

Table 3. Membrane and Bending Stresses at Midpoint of Edge (Perpendicular to Edge) versus Pressure

| | Hoffman | | Levy | |
|---|---|---|---|---|
| $p^*$ | $\frac{\sigma' a^2}{E h^2}$ | $\frac{\sigma'' a^2}{E h^2}$ | $\frac{\sigma' a^2}{E h^2}$ | $\frac{\sigma'' a^2}{E h^2}$ |
| 17.79 | .0884 | 4.8263 | .12 | 5.36 |
| 38.3 | .3568 | 9.8551 | .47 | 11.05 |
| 63.4 | .8001 | 15.0926 | 1.06 | 16.97 |
| 95.0 | 1.4181 | 20.5936 | 1.87 | 23.45 |
| 134.9 | 2.2172 | 26.3746 | 2.92 | 30.6 |
| 184.0 | 3.190 | 32.3220 | 4.23 | 38.2 |
| 245.0 | 4.3646 | 38.5322 | 5.78 | 47.0 |
| 318.0 | 5.7188 | 44.8158 | 7.60 | 56.3 |
| 402.0 | 7.2128 | 50.9901 | 9.64 | 66.2 |

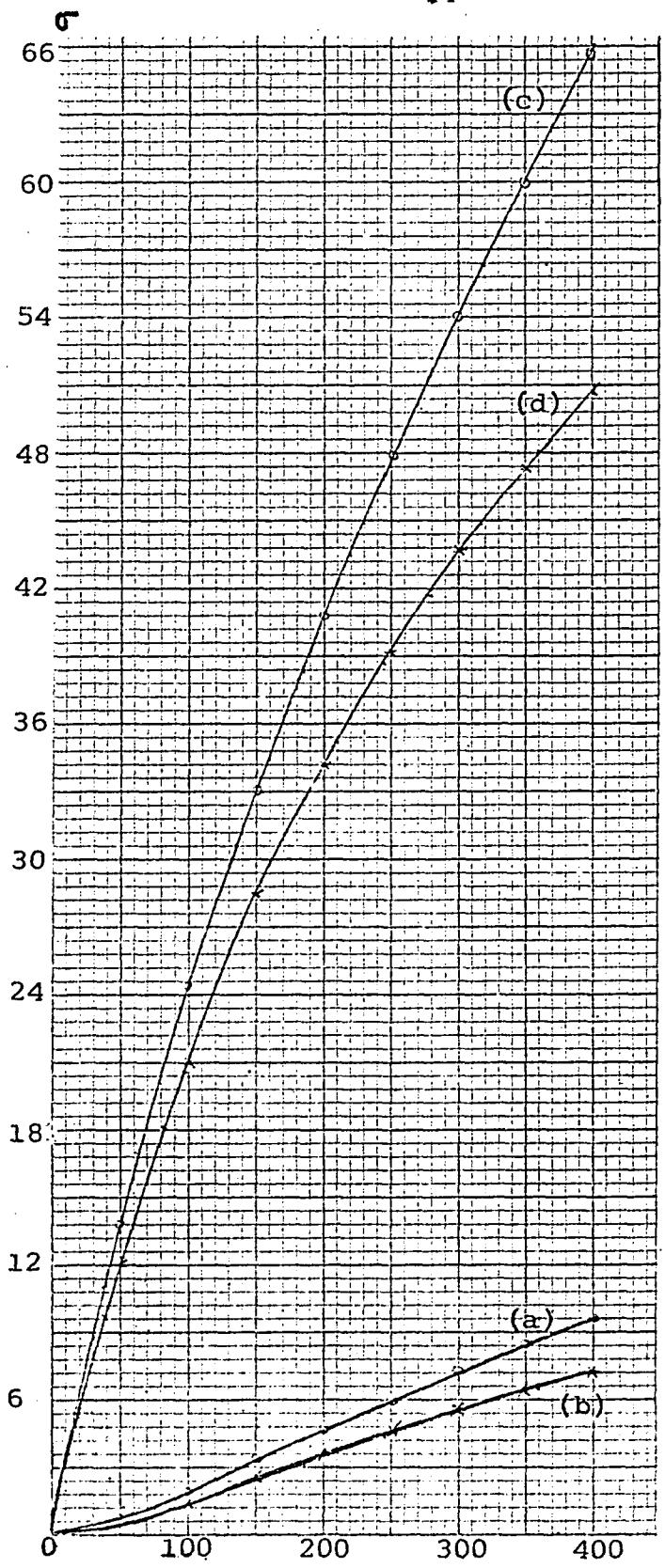


Figure 3.

Membrane and Bending Stresses at Midpoint of Edge (Perpendicular) versus Pressure

(a)
Levy: Membrane Stress

(b)
Hoffman: Membrane Stress

(c)
Levy: Bending Stress

(d)
Hoffman: Bending Stress

Table 4. Fixed Edge: Hoffman (Two Modes) and Levy Central Deflection versus Pressure

| p* | Hoffman | Levy |
|---|---|---|
| 17.79 | .2361 | .237 |
| 38.3 | .4699 | .471 |
| 63.4 | .6937 | .695 |
| 95.0 | .9070 | .912 |
| 134.9 | 1.1111 | 1.121 |
| 184.0 | 1.3045 | 1.323 |
| 245.0 | 1.4930 | 1.521 |
| 318.0 | 1.6735 | 1.714 |
| 402.0 | 1.8433 | 1.902 |

Figure 4. Fixed Edge: Hoffman (Two Modes) and Levy Central Deflection versus Pressure

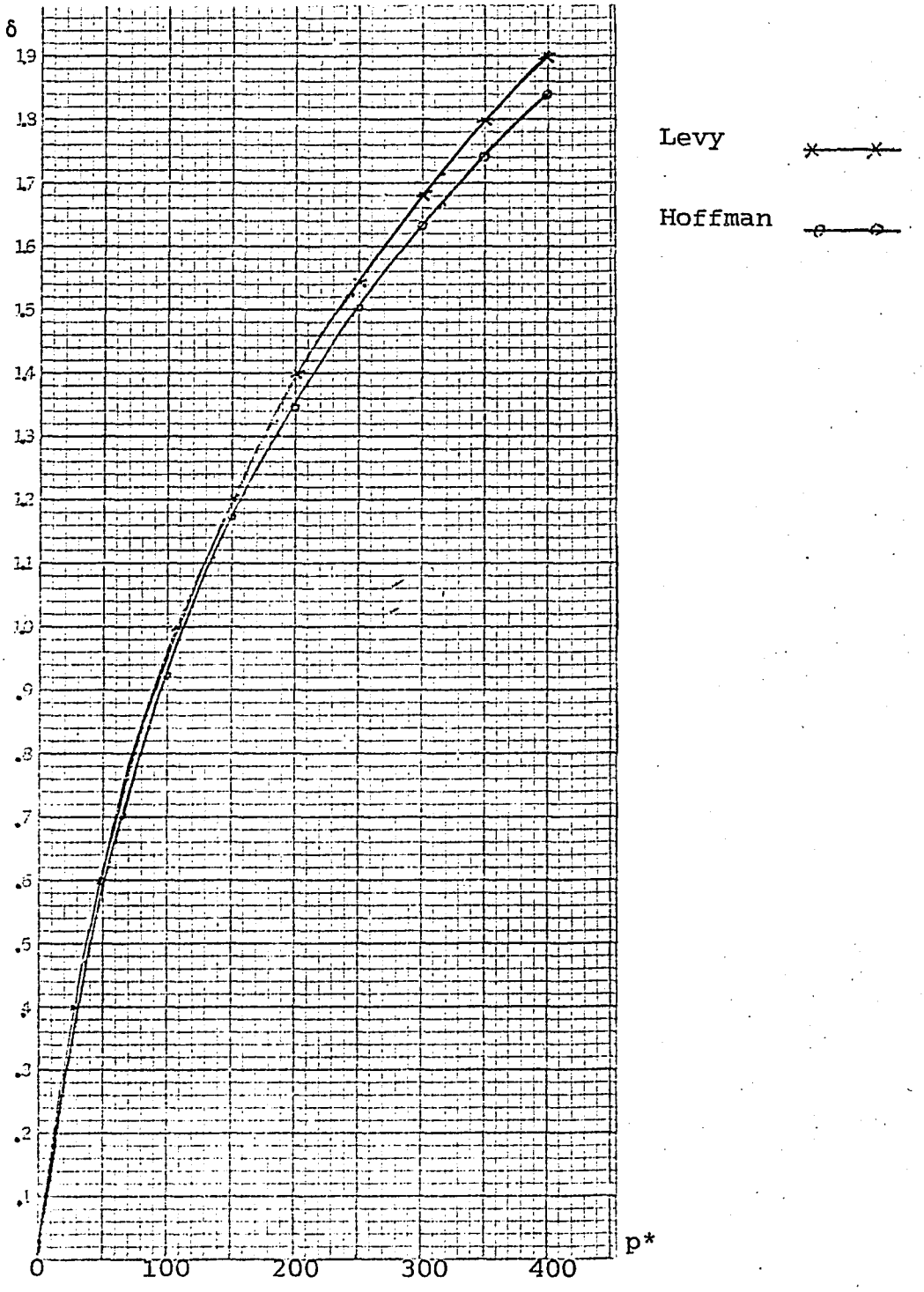

Table 5. Shape of Deflected Plate Along $y = \frac{1}{2}a$ at $p^* = 402$

Note: Plate is symmetric with respect to $x = .5\,a$

| x | Hoffman | Levy | Vol'mir |
|---|---|---|---|
| 0 | 0 | 0 | 0 |
| .05 a | .1024 | .1193 | .0475 |
| .10 a | .3556 | .3976 | .1855 |
| .15 a | .6827 | .7243 | .4004 |
| .20 a | 1.0175 | 1.0287 | .6712 |
| .25 a | 1.3118 | 1.3002 | .9714 |
| .30 a | 1.5391 | 1.5099 | 1.2716 |
| .35 a | 1.6936 | 1.6789 | 1.5424 |
| .40 a | 1.7851 | 1.8023 | 1.7573 |
| .45 a | 1.8302 | 1.8753 | 1.8953 |
| .50 a | 1.8433 | 1.902 | 1.943 |

Figure 5. Shape of Deflected Plate Along $y = \frac{1}{2}a$ at $p^* = 402$

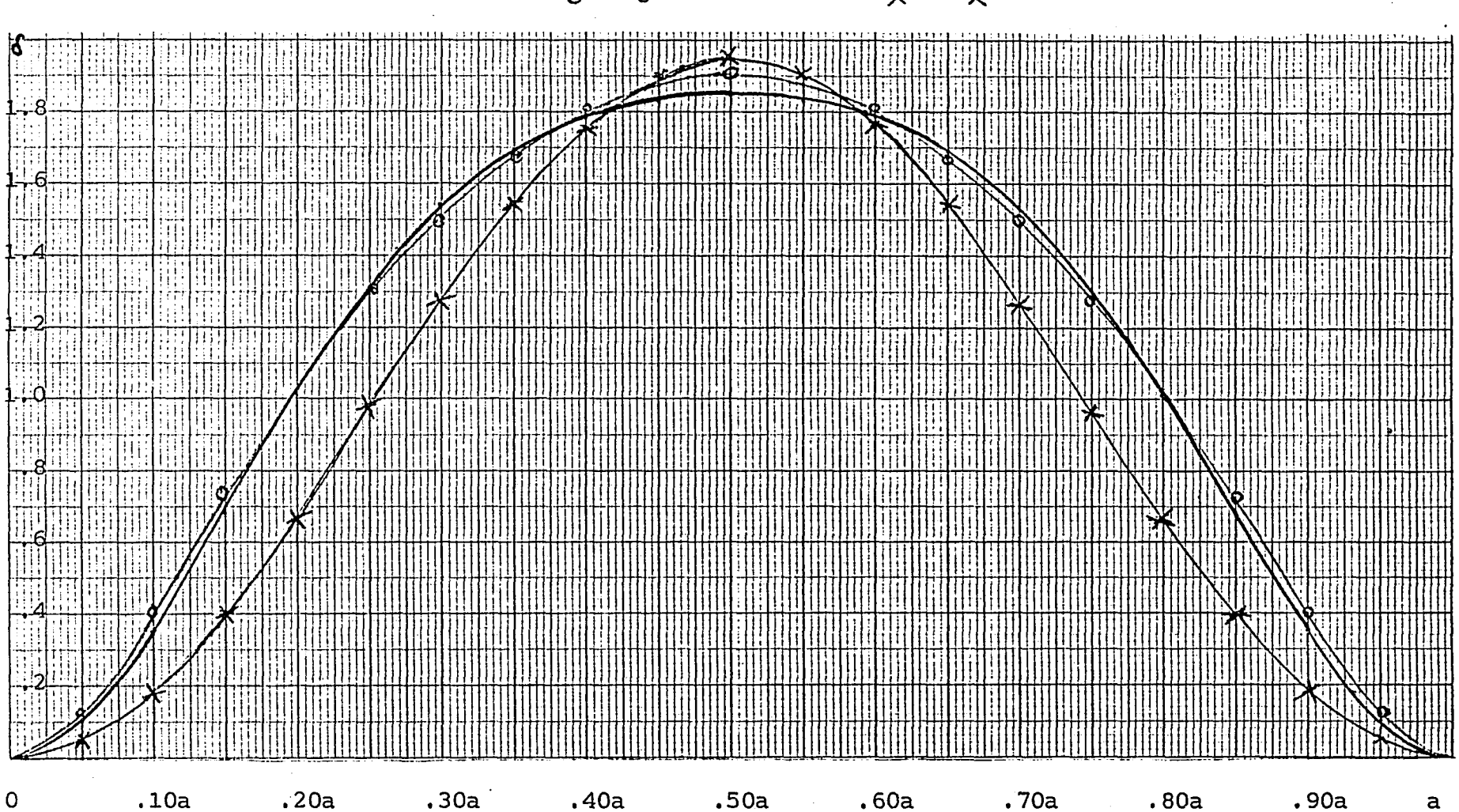

Table 6. Fixed Edge: One and Two Mode Bending Stresses versus Pressure

| $p^*$ | One Mode $\frac{\sigma'' a^2}{E h^2}$ | Two Mode $\frac{\sigma'' a^2}{E h^2}$ |
|---|---|---|
| 17.79 | 3.6411 | 4.8263 |
| 38.3 | 7.1878 | 9.8551 |
| 50.0 | 9.0006 | 12.4116 |
| 63.4 | 10.9357 | 15.0926 |
| 80.0 | 13.1650 | 18.1084 |
| 95.0 | 15.0506 | 20.5936 |
| 134.9 | 18.6406 | 26.3746 |
| 184.0 | 22.0325 | 32.3220 |
| 210.0 | 23.5589 | 35.1007 |
| 245.0 | 25.4043 | 38.5322 |
| 280.0 | 27.0623 | 41.6733 |
| 318.0 | 28.6940 | 44.8158 |
| 360.0 | 30.3380 | 48.0205 |
| 402.0 | 31.8459 | 50.9901 |

Figure 6. Fixed Edges: One and Two Mode Bending

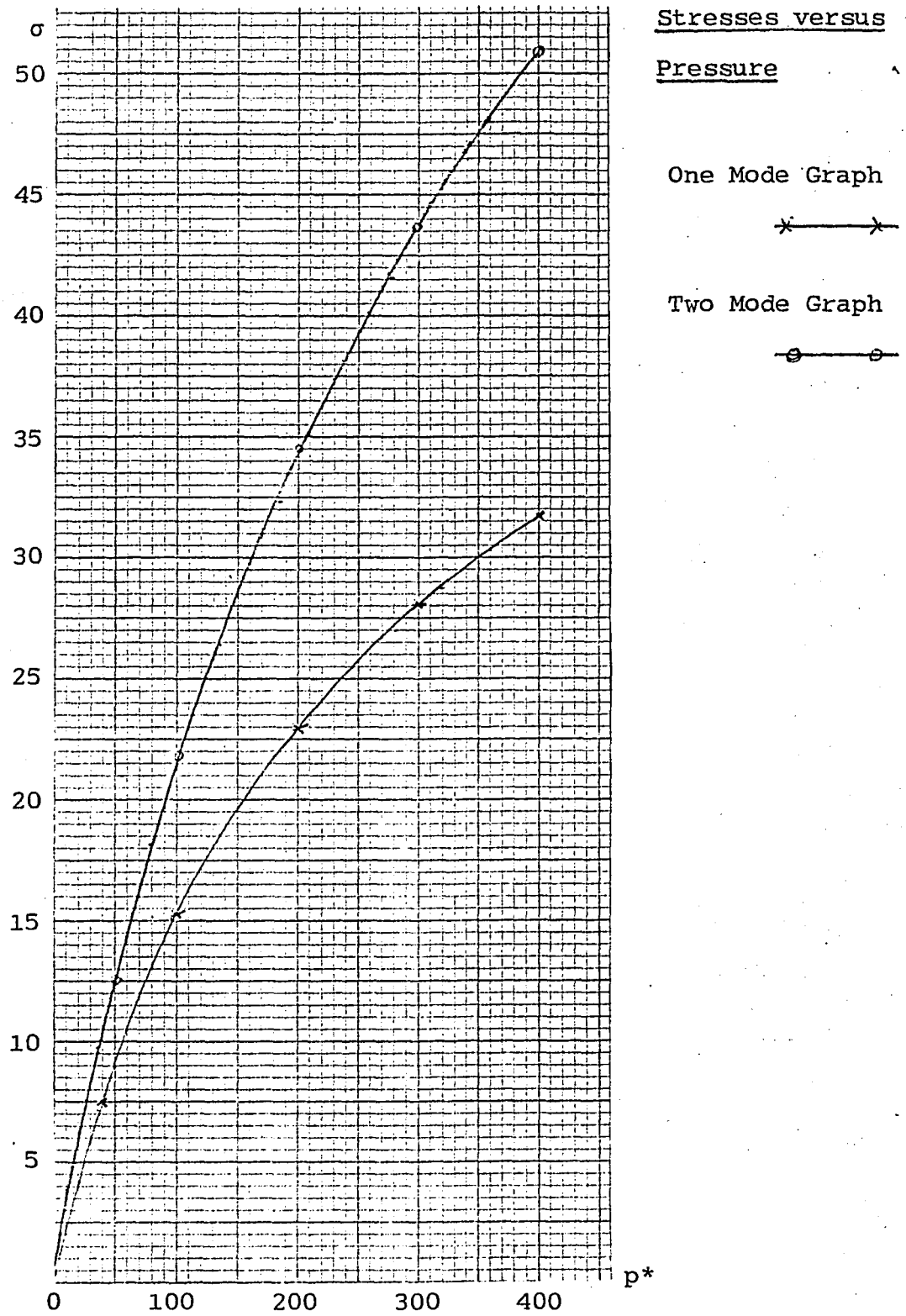

Table 7. Integrals

| | | | | |
|---|---|---|---|---|
| (1) | = | $\int_0^a u_1(x)u_1''(x)\,dx$ | = | $-.218015215\,a$ |
| (2) | = | $\int_0^a [u_1'(x)]^2 dx$ | = | $.218015215\,a$ |
| (3) | = | $\int_0^a [u_1(x)]^2 u_1''(x)\,dx$ | = | $-.21357625\,a$ |
| (4) | = | $\int_0^a [u_1''(x)]^2 u_1(x)\,dx$ | = | $.165938494\,a$ |
| (5) | = | $\int_0^a [u_1(x)]^3 u_1''(x)\,dx$ | = | $-.198226036\,a$ |
| (6) | = | $\int_0^a u_3(x)\,dx$ | = | $-.258726749\,a$ |
| (7) | = | $\int_0^a [u_3(x)]^2 dx$ | = | $.505859962\,a$ |
| (8) | = | $\int_0^a [u_3(x)]^3 dx$ | = | $-.209407206\,a$ |
| (9) | = | $\int_0^a [u_3(x)]^4 dx$ | = | $.418772309\,a$ |
| (10) | = | $\int_0^a u_3(x)u_3''(x)\,dx$ | = | $-.41381783\,a$ |
| (11) | = | $\int_0^a [u_3'(x)]^2 dx$ | = | $.41381783\,a$ |
| (12) | = | $\int_0^a [u_3(x)]^2 u_3''(x)\,dx$ | = | $.139595437\,a$ |
| (13) | = | $\int_0^a [u_3''(x)]^2 u_3(x)\,dx$ | = | $-.1047036\,a$ |
| (14) | = | $\int_0^a [u_3(x)]^3 u_3''(x)\,dx$ | = | $-.362871230\,a$ |
| (15) | = | $\int_0^a u_1(x)u_3(x)\,dx$ | = | 0 |
| (16) | = | $\int_0^a u_1(x)u_3''(x)\,dx$ | = | $-.036044115\,a$ |
| (17) | = | $\int_0^a u_3(x)u_1''(x)\,dx$ | = | $-.19477943\,a$ |

Table 7. (continued)

| | | | | |
|---|---|---|---|---|
| (18) | = | $\int_0^a u_1'(x)u_3'(x)\,dx$ | = | .083789332 a |
| (19) | = | $\int_0^a [u_3(x)]^2 u_1(x)\,dx$ | = | .286218960 a |
| (20) | = | $\int_0^a [u_1(x)]^2 u_3(x)\,dx$ | = | .082036446 a |
| (21) | = | $\int_0^a [u_3'(x)]^2 u_1(x)\,dx$ | = | .259570042 a |
| (22) | = | $\int_0^a [u_1'(x)]^2 u_3(x)\,dx$ | = | - .143863156 a |
| (23) | = | $\int_0^a u_1'(x)u_3'(x)u_1(x)\,dx$ | = | .113509324 a |
| (24) | = | $\int_0^a u_1'(x)u_3'(x)u_3(x)\,dx$ | = | .013082315 a |
| (25) | = | $\int_0^a u_3''(x)[u_1(x)]^2 dx$ | = | - .097657853 a |
| (26) | = | $\int_0^a u_1''(x)[u_3(x)]^2 dx$ | = | - .060823155 a |
| (27) | = | $\int_0^a u_1''(x)u_1(x)u_3(x)\,dx$ | = | - .120004340 a |
| (28) | = | $\int_0^a u_3''(x)u_1(x)u_3(x)\,dx$ | = | - .265197733 a |
| (29) | = | $\int_0^a [u_1(x)]^2[u_3(x)]^2 dx$ | = | .205722939 a |
| (30) | = | $\int_0^a [u_3(x)]^2 u_1''(x)u_1(x)\,dx$ | = | - .102576275 a |
| (31) | = | $\int_0^a [u_1(x)]^2 u_1''(x)u_3(x)\,dx$ | = | -.110654941 a |
| (32) | = | $\int_0^a [u_1(x)]^3 u_3(x)\,dx$ | = | .115281079 a |
| (33) | = | $\int_0^a [u_1(x)]^3 u_3''(x)\,dx$ | = | - .124970479 a |
| (34) | = | $\int_0^a [u_1(x)]^2 u_3''(x)u_3(x)\,dx$ | = | - .199313656 a |

Table 7. (continued)

| | | | | |
|---|---|---|---|---|
| (35) | = | $\int_0^a [u_3(x)]^2 u_3''(x) u_1(x)\, dx$ | = | - .006151134 a |
| (36) | = | $\int_0^a [u_3(x)]^3 u_1(x)\, dx$ | = | - .016161021 a |
| (37) | = | $\int_0^a [u_3(x)]^3 u_1''(x)\, dx$ | = | - .125472847 a |
| (38) | = | $\int_0^a u_1(x)\, dx$ | = | .523164360 a |
| (39) | = | $\int_0^a [u_1(x)]^2 dx$ | = | .396477920 a |
| (40) | = | $\int_0^a [u_1(x)]^3 dx$ | = | .331876988 a |
| (41) | = | $\int_0^a [u_1(x)]^4 dx$ | = | .291108371 a |
| (42) | = | $\int_0^a [u_1'(x)]^2 u_1(x)\, dx$ | = | .106788125 a |
| (43) | = | $\int_0^a [u_3'(x)]^2 u_3(x)\, dx$ | = | - .069797718 a |
| (44) | = | $\int_0^a u_1''(x) u_3''(x) u_1(x)\, dx$ | = | .115994313 a |
| (45) | = | $\int_0^a u_1''(x) u_3''(x) u_3(x)\, dx$ | = | .10384758 a |
| (46) | = | $\int_0^a u_3(x) [u_1''(x)]^2\, dx$ | = | .026216524 a |
| (47) | = | $\int_0^a u_1(x) [u_3''(x)]^2\, dx$ | = | .252685394 a |

## BIBLIOGRAPHY

[1] Lord Rayleigh, The Theory of Sound, Volume I, Second Edition, New York, Dover, 1945.

[2] Stuart Way, Uniformly Loaded, Clamped, Rectangular Plates With Large Deflection, Proceedings of the Fifth International Congress of Applied Mechanics (Cambridge, Mass., 1938), John Wiley and Sons Inc., 1939, pp. 123-128.

[3] Samuel Levy, Square Plates With Clamped Edges Under Normal Pressure Producing Large Deflections, Report No. 740, National Advisory Committee for Aeronautics, 1942.

[4] A. S. Vol'mir, Flexible Plates and Shells, Translated by Department of Engineering Science and Mechanics, University of Florida, Technical Report AFFDL-TR-66-216, Air Force Flight Dynamics Laboratory, Research and Technology Division, Air Force Systems Command, Wright-Patterson Air Force Base, Ohio, April 1967.

[5] A.E.H. Love, A Treatise on the Mathematical Theory of Elasticity, Fourth Edition, New York, Dover, 1944.

[6] J.J. Stoker, Non-linear Elasticity, New York, Gordon and Breach, 1968.

[7] M.R. Spiegel, Mathematical Handbook of Formulas and Tables, Schaum's Outline Series, New York, McGraw-Hill, 1968.

[8] Samuel Levy, Bending of Rectangular Plates With Large Deflections, Report No. 737, National Advisory Committee for Aeronautics, 1942.

[9] S. Levy, W. Ramberg, A.E. McPherson, Normal Pressure Tests of Rectangular Plates, Report No. 748, National Advisory Committee for Aeronautics, 1942.